Temporal and Spatial Epigenome Editing Allows Precise Gene Regulation in Mammalian Cells

Cem Kuscu [1], Rashad Mammadov [1], Agnes Czikora [1], Hayrunnisa Unlu [5], Turan Tufan [1], Natasha Lopes Fischer [1], Sevki Arslan [2], Stefan Bekiranov [1], Masato Kanemaki [3,4] and Mazhar Adli [1]

*1 - **Department of Biochemistry and Molecular Genetics,** School of Medicine, University of Virginia, Charlottesville, VA 22908, USA*
*2 - **Department of Biology,** Pamukkale University, Denizli, 20160, Turkey*
*3 - **National Institute of Genetics and SOKENDAI,** Mishima, Sizuoka, 411-8540, Japan*
*4 - **PRESTO,** Japan Science and Technology Agency, Kawaguchi, Saitama 332-0012, Japan*
*5 - **School of Medicine,** Ankara University, Ankara, 06560, Turkey*

***Correspondence to Mazhar Adli:** Department of Biochemistry and Molecular Genetics, School of Medicine, University of Virginia, Charlottesville, VA 22908, USA. adli@virginia.edu*
https://doi.org/10.1016/j.jmb.2018.08.001
Edited by Stanley Qi

Abstract

Cell-type specific gene expression programs are tightly linked to epigenetic modifications on DNA and histone proteins. Here, we used a novel CRISPR-based epigenome editing approach to control gene expression spatially and temporally. We show that targeting dCas9–p300 complex to distal non-regulatory genomic regions reprograms the chromatin state of these regions into enhancer-like elements. Notably, through controlling the spatial distance of these induced enhancers (i-Enhancer) to the promoter, the gene expression amplitude can be tightly regulated. To better control the temporal persistence of induced gene expression, we integrated the auxin-inducible degron technology with CRISPR tools. This approach allows rapid depletion of the dCas9-fused epigenome modifier complex from the target site and enables temporal control over gene expression regulation. Using this tool, we investigated the temporal persistence of a locally edited epigenetic mark and its functional consequences. The tools and approaches presented here will allow novel insights into the mechanism of epigenetic memory and gene regulation from distal regulatory sites.

Introduction

Identifying *cis*-regulatory elements in the genome enabled better understanding of cell-type specific gene expression programs during normal differentiation and disease progression. Proximal elements such as promoters and distal elements such as enhancers, locus control regions, silencers, and insulators have been identified as regulatory elements that control spatial and temporal gene expression [1]. Dynamic deposition and removal of epigenetic marks at these regulatory genomic regions during differentiation are tightly associated with normal development and lineage-specific transcriptional programs [2]. Large-scale epigenome mapping efforts such as ENCODE [3] and REMC [4] projects have shed unprecedented lights on distributions of various chromatin marks across the genome [4–6]. Chromatin landscapes from these studies also served as reference points to identify disease-specific aberrant epigenomic features. Abnormal deposition of epigenetic information at regulatory genomic elements due to mutations in epigenetic modifiers is a hallmark of multiple developmental diseases, including cancer [7–10]. Excitingly, the reversible nature of the epigenome offers the opportunity that disease-associated anomalous gene expression can be epigenetically reprogrammed. Therefore, the idea of reprogramming the epigenome by small-molecule epigenetic inhibitors or more precisely through locus-specific epigenome editing tools such as the CRISPR or TALEN approaches has immediate therapeutic implications.

Recent progress in CRISPR-based epigenome editing now offers unprecedented power to study the

functional role of various chromatin modifications [11]. In the type II CRISPR system, the Cas9 endonuclease protein is guided to a specific genomic region via a short-guide RNA (sgRNA). Upon targeting, WT Cas9 introduces DNA double-strand breaks, whereas catalytically inactive Cas9 (dCas9) can bind to the target DNA region without causing any breaks [12–14]. Exploiting this unique feature, dCas9 has been repurposed for a wide range of applications such as gene regulation [15–17], live cell chromatin imaging [18,19], and genome-scale screens through gene activation and repression [20]. In addition to these instrumental biological tools, dCas9-based targeting approaches now allow locus-specific epigenome editing [21–23]. This is achieved by coupling catalytically inactive dCas9 with effector domains of epigenetic modifiers. For example, dCas9–p300 fusion complex has been utilized to specifically activate gene expression from a targeted promoter or enhancer region [21]. On the other hand, dCas9–LSD1 [23], dCas9–KRAB [22], and dCas9–DNMT3A [24] fusion complexes have been targeted to specific promoters or enhancer regions to manipulate local chromatin modifications and dampen gene expression.

Posttranslational modifications on histone proteins are associated with distinct activities of regulatory elements in the genome [4,25]. For example, accumulation of H3K27ac and higher H3K4me1 (2)/H3K4me3 ratio in addition to the transcription factors binding and DNase I hypersensitivity in the distal part of TSS define these regulatory elements as an enhancer. Enhancers are genomic regulatory elements that mediate cell type-specific gene expression from promoter distal sites [26–28]. Genome-wide ChIP-Seq and DNase hypersensitivity followed by sequencing suggest that there are 500,000 to 1.5 million potential distal regulatory sites in the human genome [4,29,30]. Notably, aberrant regulatory activity from distal enhancers is now being increasingly recognized as the cause of various diseases, including cancer [31–34]. Our mechanistic understanding of exactly how an enhancer element regulates the promoter activity and gene expression from a long, linear distance away is limited. The conventional working model is that transcription factors first bind to the enhancer elements and recruit additional transcriptional co-activators and chromatin-modifying complexes to enhance gene expression. P300 is a transcriptional co-activator that is being recruited to enhancer and promoter elements by specific transcription factors. Since dCas9-mediated targeted recruitment of p300 complex is able to induce gene expression from known enhancer elements [21], we hypothesize that targeted recruitment of the dCas9–p300 complex to a non-regulatory distal region will override the necessity of the initial binding of a transcription factor binding and will be sufficient to reprogram the region into an enhancer-like element. CRISPR-based epigenome editing approaches enable selective deposition of an epigenetic mark at the target site resulting in gene activation or repression [21,23]. However, it remains a major challenge to establish the causal relationship between the presence of a histone mark and the local regulatory activity of the associated genetic element. Current platforms have two major limitations in overcoming this aforementioned challenge. First, the dCas9-fused epigenetic modifiers, such as p300 and repressive KRAB domain, have additional roles than just modifying the histones including recruitment of transcriptional activators or repressors. Second, the fusion complex remains associated with the target site. Thus, the physical presence of the fusion complex at the target site further confounds the experimental conclusion regarding the functional relevance of the edited epigenetic mark and the observed biological outcome.

Here, we present next-generation CRISPR-based epigenome editing tool that will enable better mechanistic understanding of the functional roles of epigenetic marks. Initially, we show that the dCas9–p300 complex can epigenetically reprogram a non-regulatory genomic region into an enhancer-like element, which we call induced enhancers [i-Enhancer (iE)]. More importantly, our results demonstrate that by controlling the distance between iEs and the promoter, the relative intensity of gene expression can be controlled. Moreover, by adopting the auxin-inducible degron (AID) technology, we devised an original targeting approach where the dCas9-fused epigenetic modifier can be degraded acutely from the target sites. This approach enables better interrogation of the functional roles and temporal persistence of locally deposited epigenetic marks on proximal and distal regulatory elements.

Results

Epigenetic reprogramming of non-regulatory distal sites into enhancer-like elements

Various epigenetic modifiers and general transcriptional activators and repressors have been fused to catalytically inactive dCas9 to achieve locus-specific epigenome manipulation and gene regulation [11]. Here, we used dCas9 fusion to a wild-type or mutant histone acetyl transferase (HAT) core domain of the p300 complex [21]. Full-length p300 is a transcriptional co-activator that has promiscuous acetyltransferase activity [35]. On chromatin, it acetylates histone 3 at lysine 27 position (H3K27ac), which is an epigenetic mark of active enhancers and promoters [29]. To simplify, we will call the dCas9–$p300^{HAT}$ and dCas9–$p300^{HAT\text{-}mutant}$ fusion complexes as dCas9–p300 and dCas9–p300-mut, respectively, throughout this manuscript. We started this study by aiming to test a hypothesis that local recruitment of epigenetic modifiers and transcriptional activators such as p300 will reprogram non-regulatory distal sites into functional

genomic elements (Fig. 1a). To test this hypothesis, we targeted the dCas9–p300 complex to multiple regions distal to the *IL1RN* promoter. We specifically targeted regions approximately 4, 8, and 24 kb from the *IL1RN* promoter that do not contain any feature of a regulatory element based on ENCODE H3K27ac and transcription factor ChIP-Seq data (Figs. 1b and S1a). Initially, we performed luciferase reporter assays to confirm that our target sites have no regulatory roles in the HEK293T and K562 cells. To do this, we PCR amplified ~300-bp DNA fragments around the sgRNA target sites from the *IL1RN* gene promoter as well as from three distal targeting regions and cloned them into luciferase reporter plasmids. The assay indicated significant luciferase activity only from the promoter; none of the distal targeting DNA elements induced luciferase gene expression (Fig. 1c). We further tested the role of iEs in the luciferase plasmid that has SV40 promoter. These DNA fragments did not show any contributions to the luciferase activity induced by promoter (Fig. S2). Then we checked to see if targeting dCas9– p300 complex to these regions would increase H3K27ac levels and gene expression. Notably, the recruitment of dCas9–p300 resulted in a significant increase in H3K27ac level at each of the distal target sites, suggesting that the local increase in H3K27ac is not limited to known regulatory elements such as enhancers and promoters (Figs. 1d and S3). Importantly, the quantitative ChIP-qPCR measurements show that the recruitment of dCas9–p300 complex to any of the distal region also resulted in significant increase in H3K27ac at the promoter site (last column in Fig. 1d; *p* values iE1 = 0.0132; iE2 = 0.0198; iE3 = 0.0016 with an unpaired *t*-test). Interestingly, this suggests that targeting dCas9–p300 complex to a non-regulatory distal genomic site results in increased epigenetic editing not only at the target site but also at the promoter region that is as far as 24 kb distal to the target site. We then tested to see if local increase in H3K27ac at the iEs and the promoter regions is correlated with the *IL1RN* gene expression induction. We observed the highest gene expression induction from targeting the promoter region as we expected and a significant increase in gene expression from modifying each of the iE elements in 293T cells (Fig. 1e, left). We detected an inverse correlation between the iE distance to the promoter and the level of induced gene expression (Fig. S4a). These results

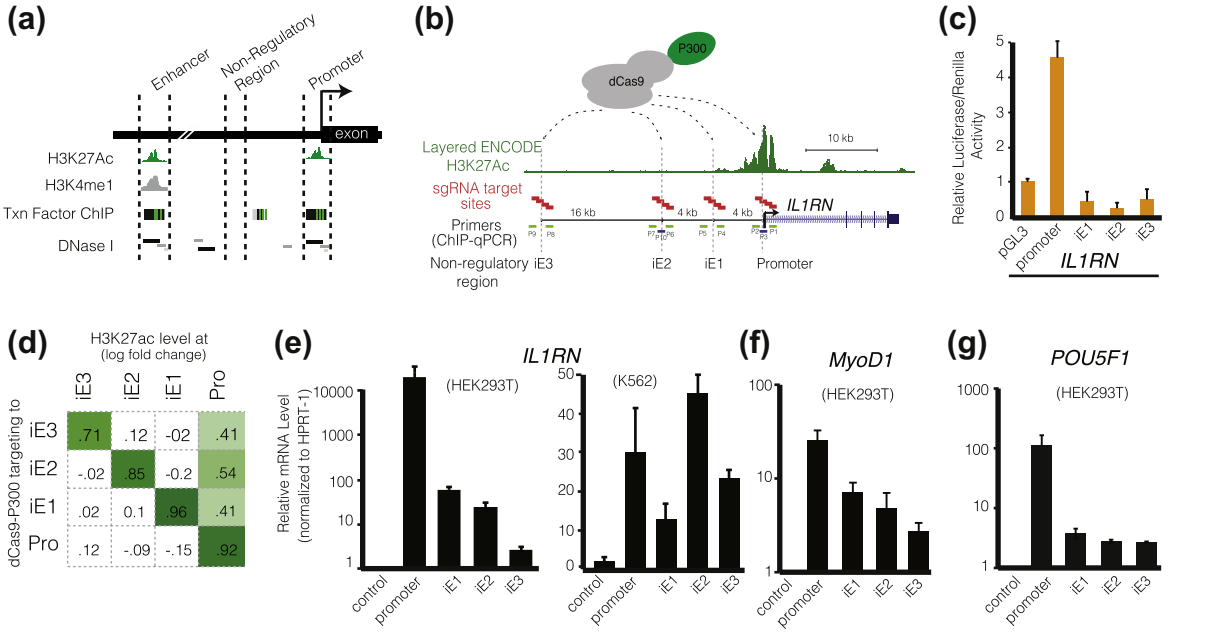

Fig. 1. Spatial control of gene expression through epigenetic reprogramming of induced enhancer (iE) elements. (a) Schematics summarize gene proximal promoter and distal enhancer DNA elements where transcription factors bind and histone marks accumulate. (b) H3K27ac chromatin state of IL1RN locus is shown based on layered ENCODE data. The schematics of the promoter and iE targeting sgRNA and ChIP-qPCR primer sites are indicated with red and green bars, respectively. (c) Relative luciferase activity is measured for each of the iE element and the promoter region. The results are normalized to internal Renilla activity. The luciferase activity is based on average signal intensity of three independent experiments. (d) Log-transformed average H3K27ac levels are shown in a heat map for promoter and three iE sites. Error bars are standard errors of means of at least three independent experiments. Actual H3K27ac enrichment levels are shown in supplementary Fig. 3. (e–g) mRNA levels (RT-qPCR) are shown after targeting dCas9–p300 to each of the indicated regions in the IL1RN (e), MyoD1 (f), and POU5F1 (g) locus. Two different cell types were used for IL1RN loci. HPRT-1 gene is used for normalization of RT-qPCR, and GFP-sgRNA is used as a control. Error bars are standard error of means of at least three independent experiments.

suggest that targeting the dCas9– p300 complex epigenetically reprogrammed the non-regulatory distal elements into artificially induced enhancer-like elements, the iEs.

To further understand whether this is a locus-specific observation or not, we tested analogous targeting approach on multiple other genomic loci in a 293T cell line. Like *IL1RN* locus, we specifically targeted regions that do not contain any epigenomic features of a potential regulatory element (Fig. S1b, c). H3K27ac ChIP experiments on *MYOD1* and *POU5F1* loci suggest a consistent trend as the *IL1RN* locus where targeting distal iEs resulted in a significant increase in H3K27ac level at each of the target sites (Figs. S5 and S6). Notably, like *IL1RN* promoter and iE elements, results from *MYOD1* (Fig. 1f) and *POU5F1* (also known as *OCT4*) loci (Fig. 1g) suggest highly comparable trends in iE-mediated gene expression induction in 293T cells. For the *MYOD1* locus in 293T cells, we again find a trend comparable to the *IL1RN* locus but with a slower decay of gene expression as the spatial distance of the target site from the promoter increases (Fig. S4b). To further understand if the induced enhancers could be established in other cell types as well, we targeted *IL1RN* locus in K562 cell line. Like 293T cells, we observed strong *de novo* induced acetylation at all iE sites at the *IL1RN* locus. We also detected significant gene induction from all iE sites in K562 cells; however, we did not observe an exponential relationship between the iE-promoter distance and gene expression (Fig. 1e, right).

The data in which iE targeting results in increased H3K27ac not only at the target site but also at the promoter region located 24 kb away (Fig. 1d) led to the hypothesis that the targeted iE forms a chromatin loop with the promoter region upon targeting with dCas9–p300. To test this, we performed quantitative chromosome conformation capture (3C) assays to detect any interaction between the iE sites and the *IL1RN* promoter site in 293T cells. The 3C method is a proximity ligation-based assay that enables identification of physical interactions between two known genomic sites [36]. We designed specific primer pairs to amplify the ligated DNA composed of the promoter and the targeted iE element (Fig. 2a). In this experiment, we also used the dCas9–p300-mut as a negative control, which does not induce *IL1RN* gene expression from distal elements (Fig. S7). Notably, when we targeted the dCas9–p300 to the iE-2 site, we observed a significant increase in 3C signal with primer pair B, which amplifies a looped DNA segment between the iE-2 site and the promoter. This interaction is specifically detected when the catalytically active dCas9–p300 complex is targeted. The dCas9–p300-mutant complex resulted in a background level 3C signal (Fig. 2b). We observed comparable results when

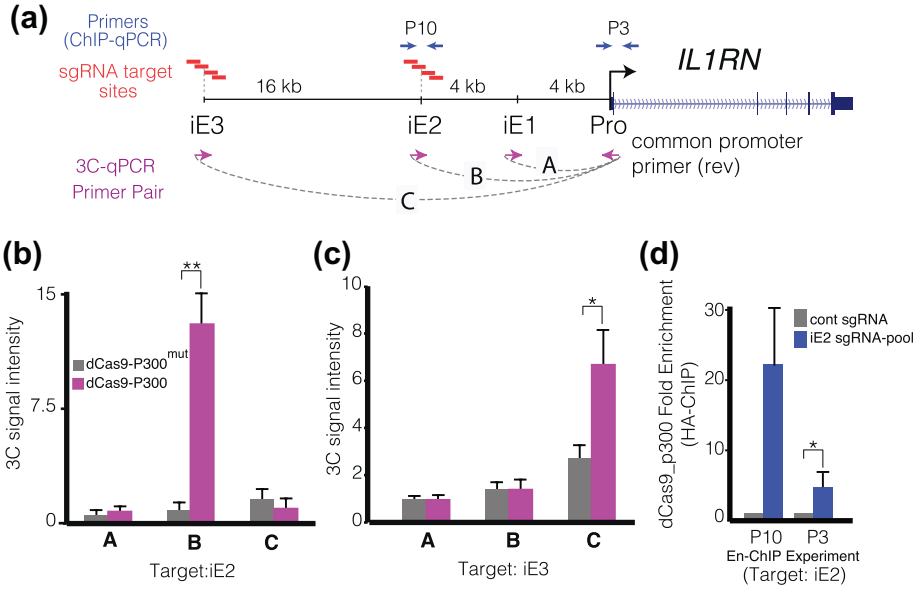

Fig. 2. Epigenetic reprogramming of distal iEs induces 3D conformational changes and chromatin looping. (a) Three different primer pairs used for the 3C assay are shown on the diagram. Common promoter primer of IL1RN is used as a reverse primer, and separate forward primers are used for each iEs sites. (b, c) Normalized 3C signal ratios were calculated for the three potential interaction sites after local recruitment of dCas9–p300 or dCas9–p300-mut transfected cells after three independent experiments. Primers amplifying a gene desert genomic region were used as an internal genomic control. *p*-value = 0.0019 for primer pair B, *p*-value = 0.0384 for primer pair C, unpaired *t*-test. (d) The en-ChIP analysis of dCas9–p300 interaction with the promoter region after targeting the iE site. HA-tagged dCas9–p300 is targeted to iE-2 region, and HA-ChIP was performed. ChIP-qPCR-measured dCas9–p300 fold enrichment levels with indicated primers pairs are shown on the top panel. Error bars are standard error of means of at least three independent experiments.

a more distal iE-3 element was targeted (Fig. 2c). These results suggest that targeting dCas9–p300 to iE sites results in chromatin looping whereby the dCas9–p300 complex directly interacts with the promoter region and deposits the H3K27ac mark. To further support this claim that there is a direct interaction of dCas9–p300 with the promoter, we used the engineered DNA-binding molecule-mediated chromatin immunoprecipitation (enChIP) method [37]. Here, we specifically targeted the HA-tagged dCas9–p300 complex to the iE-2 region and performed ChIP with anti-HA antibody to identify the genomic regions that are associated with the complex. We recently used this approach to identify genome-level targeting specificities of CRISPR/Cas9 [38]. Notably, the ChIP-qPCR results presented in Fig. 2d show more than 20-fold enrichment (with primer pair 10) of this complex at the target site (iE2). More importantly, we also observed a significant enrichment of dCas9–p300 at the promoter region as well, indicating a direct interaction of iE2 target region with the promoter and hence chromatin looping between these two sites located 8 kb away from each other.

In conclusion, these results suggest that non-regulatory genomic regions can be targeted and epigenetically reprogrammed to function like a typical enhancer site. This targeting approach results in locus-specific manipulation of epigenetic marks and conformational changes in chromatin structure. Such spatial targeting of non-regulatory genomic regions allows tighter regulation of relative gene expression induction and potentiates mechanism of enhancer–promoter interactions and enhancer-mediated gene activation.

Auxin-induced degradation of the CRISPR-epigenetic writer on promoters and iE sites

In additional to spatially controlling gene expression, we also aim to advance the dCas9-epigenetic editing approach to temporally control gene expression. To this end, we exploited a plant-based AID technology [39,40] to acutely degrade the epigenetic writer in a hormone-dependent manner. In this inducible and reversible rapid protein degradation system, which is illustrated in Fig. 3a, the plant-based auxin hormones or its chemical analog indole-3-acetic acid induces rapid degradation of proteins that contain a specific "degron" called AID. The presence of auxin in the environment induces recognition of the degron by the SCF-E3 ubiquitin ligase system through the TIR1 protein. While non-plant eukaryotes lack TIR1, they share the SCF-E3 degradation pathway. Therefore, when TIR1 is expressed in mammalian cells, they become responsive to auxin hormone and immediately degrade any proteins that contain the AID degron peptide [39]. We reasoned that by fusing the AID to the engineered dCas9–chromatin modifier complex, we can specifically degrade this complex at their target regions. Thus, the approach will enable us to assess the stability of an epigenetic mark and the duration of their functional effects on gene expression. Therefore, we generated AID-tagged dCas9–p300 chromatin-modifying complexes targeted to the *IL1RN* promoter, which demonstrated the highest gene induction in our target sites so far (Fig. S8a). We initially checked that the AID–dCas9–p300 complex was functional. The chromatin immunoprecipitation (ChIP) and gene expression analysis indicated that the AID-dCas9–p300 complex can strongly bind to the target promoter (Fig. S8b) and resulted in a significant increase in local H3K27ac level (Fig. S8c; $^{**}p$ values = 0.0051, unpaired *t*-test). More importantly and in line with the increase in local H3K27ac levels, we observe a significant increase in *IL1RN* mRNA expression. Notably, because the AID–dCas9–p300 complex was transiently transfected into HEK293T cells, the induced expression of the *IL1RN* gene is progressively lost over the period of 15 days (Fig. S8d). These results are in agreement with a recent study that used the dCas9–p300 for the same gene promoter [21] and suggested that the addition of the AID degron does not interfere with the function of the complex.

We then assessed whether the complex could be efficiently depleted globally as well as from the targeted promoter region. To be able to do this, we generated HEK293T cells that express the *TIR1* gene from *Oryza sativa,* the rice plant. TIR1 is the only required protein in mammalian cells to enable auxin response and degradation of proteins that contain the AID degron [39]. Notably, we observe that AID–dCas9–p300 complex is rapidly and completely degraded from the HEK293T^{TIR1} cells (Fig. 3b). Encouraged by these findings, we wanted to utilize this auxin-induced degradable dCas9–p300 complex to target specific genomic regions and assess the persistence and functional memory of the locally deposited H3K27ac epigenetic mark. Thus, we targeted this complex via the same four sgRNAs to the *IL1RN* gene promoter and assessed the levels of epigenetic and gene expression changes immediately after removal of the dCas9–p300 complex at the target site. ChIP experiments indicate that as early as 3 h after auxin induction, there is nearly a 75% local reduction in chromatin-bound dCas9–p300 complex (writer) at the *IL1RN* gene promoter, and the reduction was around 90% within the first 6 h of auxin induction. By 12 h, there was barely any detectable dCas9–p300 complex in the targeted region as measured by ChIP-qPCR (Fig. 3c). Interestingly, the temporal kinetics of histone marks (H3K27ac) was much slower than the temporal kinetics of epigenetic modifier complex (p300). We observed an initial 30%–40% reduction in H3K27ac levels in the first few hours; however, we did not see any further decrease in H3K27ac for the next 24 h after auxin induction. Notably, after 24 h, there was further ~50% reduction in the locally deposited H3K27ac levels, suggesting that the reduction in H3K27ac marks is coupled with initial active de-acetylation and

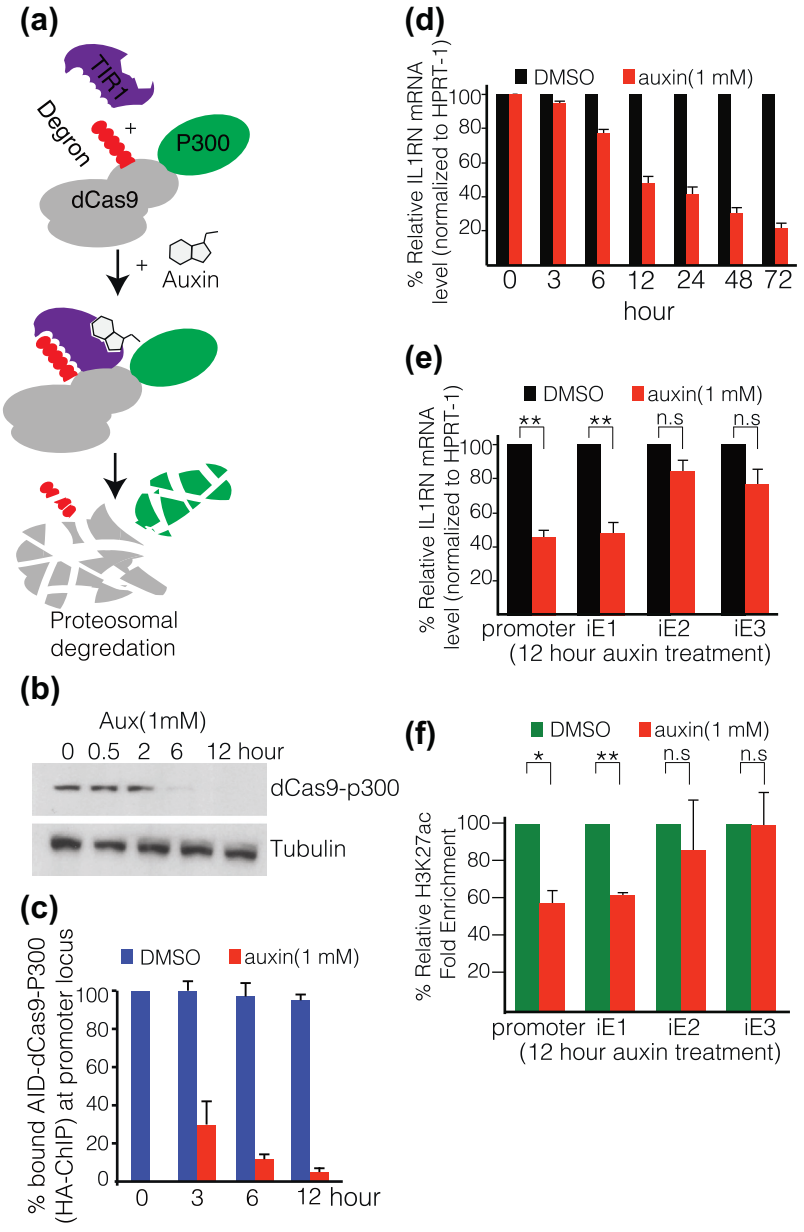

Fig. 3. Temporal epigenome editing through auxin-induced degradation. (a) The overall schematic CRISPR/Cas9 integrated AID system. (b) Western blot demonstrates total protein levels of AID–dCas9–p300 before and after induction with 1 mM of auxin by using anti-HA antibody. (c) Percent levels of changes in chromatin-bound AID–dCas9–p300 are shown on a local *IL1RN* promoter locus. (d) Bar graphs show relative *IL1RN* mRNA levels after auxin treatment for indicated times at promoter targeting. (e, f) Effects of 12-h Auxin treatment on *IL1RN* mRNA level (e) and local H3K27ac mark (f) that are induced by targeting promoter and indicated iE sites (1–3). GFP controls are not shown because of percent representation. Error bars are standard error of means of three independent experiments.

then passive dilution of the mark during mitotic transmission (Fig. S8e). The analysis of *IL1RN* mRNA levels indicated a reduction comparable to H3K27ac levels. Significantly, we observed 50% reduction in the gene expression at the 12-h time point, when nearly all local dCas9–p300 fusion complexes are degraded at the target site after auxin treatment (Fig. 3d).

Using this novel tool, we aimed to investigate whether the deposited mark has a differential rate of temporal persistence at the iE *versus* the promoter region. We therefore, targeted AID–dCas9–p300 construct to the iE sites and promoter of *IL1RN* gene in HEK293T cells where we observed robust editing and gene expression manipulation. To this end, we chose to study the effects after 12-h auxin treatment because it is the earliest time point where we observe the strongest effect of acute p300 depletion on both local histone mark and mRNA levels (Fig. 3c, d). Interestingly, auxin treatment resulted in significant reduction of *IL1RN* gene expression only when the iE1 site was targeted. In contrast, at the iE2 and iE3 sites, 12-h auxin treatment did not result in a significant decrease in gene expression (Fig. 3e). This observation suggested that local levels of the H3K27ac at these sites (iE2, 3) may not have changed following auxin treatment. Importantly, our ChIP-qPCR results showed significant reduction of histone marks at the promoter

and iE1 site. However, at the more distal iE2 and iE3 sites, we did not see a significant reduction of H3K27ac levels following auxin treatment (Fig. 3f). Taken together, these results suggest that *de novo* deposited histone marks may have differential persistency depending on where in the genome they are deposited. Our results suggest that at the main regulatory sites such as promoters, there is more dynamic remodeling of histones and hence faster removal of locally deposited histone marks than the distal iE sites.

Discussion

Epigenome editing tools will be instrumental to understand the link between chromatin modifications and regulation of gene expression. By enabling locus-specific manipulation, such approaches will elucidate the regulatory roles of various chromatin modifications in gene regulation. Here, we have further improved the CRISPR-based epigenome-editing tools to achieve two novel functions. First, we devised a novel targeting strategy and show that CRISPR-based epigenome editing can be utilized to create artificial distal enhancer sites, which we call iEs. Our findings demonstrate that guided recruitment of dCas9–p300 to the iE elements induces a specific conformational change in chromatin structure and induces gene expression from the proximal promoter. More importantly, the data suggest that by controlling the distance of the iE to the promoter region, the amplitude of gene expression can be more tightly regulated. Such approaches are expected to provide unprecedented power to custom gene expression modulation for various purposes including cellular reprogramming, gene network analysis, and therapeutic applications. Notably, the level of gene expression induction due to locus-specific editing of H3K27ac is highly variable depending on the cell type of choice. Indeed, these results are not surprising since canonical enhancers have cell type-dependent differential regulatory activity. These results suggest that cell-type specific local chromatin structure and overall transcriptional activity at the target sites substantially impact the functional output of epigenome editing. Our results also highlighted that distal non-regulatory DNA sequences may be epigenetically reprogrammed into a regulatory genomic region which can induce a 3D conformational change.

Second, we exploited the plant-based AID system [39] to develop an epigenome editor where the persistence of the locally deposited epigenetic mark and the kinetics of its functional role can be temporally studied. We demonstrated that auxin-induced degron-tagged dCas9–p300 could be degraded efficiently after auxin induction. Thus, rapid removal of the dCas9-fused chromatin modifier complex globally and locally at the target sites represents a unique and powerful approach to studying the temporal dynamics of chromatin marks. This tool allowed us to study the epigenetic memory of H3K27ac. Our data suggest that the locally deposited H3K27ac mark by the Cas9–chromatin modifier complex is inherited through mitotic cell division; however, the levels of the deposited H3K27ac are reduced during cell division suggesting a passive dilution of the H3K27ac chromatin mark. Our findings regarding the temporal persistence of H3K27ac marks are in line with a recent study where single-cell level epigenetic memory has been evaluated by time-lapse imaging of an engineered reporter system [41]. Although very powerful, this method is limited to an exogenously integrated reporter, whereas the AID-fused dCas9 system that we developed here can potentially be used for any endogenous genomic locus. Another interesting observation is that histone marks showed different levels of persistency after complete removal of the histone modifier depending on where these histone marks are deposited. Our data imply that there is a faster kinetics for *de novo* marks on or near the transcription start site, which has higher activity with respect to the distal sites of the gene. Another advantage of this tool is the quick depletion of the chromatin modifiers. Recently, a chemically controllable dCas9-fused VP16 transcriptional activator was also used to control gene expression [42]. In comparison to this approach, the AID technology allows superior temporal dynamics because it enables depletion of the target protein within hours in contrast to days.

Controllable epigenetic editing will help us to better understand chromatin biology and epigenetic mechanisms. Recently, the Crabtree group developed a method known as Fkbp/Frb-inducible recruitment for epigenome editing by Cas9 (FIRE-Cas9) in which epigenetic modifiers can be delivered to the target site through chemical induction by rapamycin. In a comparable way to our auxin treatment, they demonstrate that the histone modifier can be removed from the target site by the addition of the FK506. This then allowed quick depletion of the histone marks such as H3K9me3 and H3K4me3 in the absence of histone writers suggesting the fast kinetics of these modifiers on their target sites [43]. Together with the FIRE-dCas9, our dCas9-Auxin tool and novel spatial targeting approach will have great utilities in deciphering the functional roles of various epigenetic marks.

In summary, the novel tool and the unique targeting strategy that we present here allow temporal and spatial epigenome editing. A combination of the two can be used to better elucidate the mechanism and memory of various modes of epigenetic regulation. Such approaches further expand the CRISPR-based epigenome editing toolbox that will be instrumental to attain a mechanistic understanding of the regulatory roles of chromatin marks and non-coding genomic regions. CRISPR/dCas9 has been successfully used to image endogenous chromatin regions [18,44,45] and manipulate long-range chromatin structure [46].

We envision that integrating the epigenome and chromatin conformation editing with imaging functionality of CRISPR/Cas9 will create a novel methodology to study functional roles of long-range chromatin conformation. Such studies can be expected to shed unprecedented light on the three-dimensional organization of genomes and its functional consequences in the nuclei of living cells.

Materials and Methods

Cell culture

DMEM media and IMDM media containing 10% fetal bovine serum and 1% penicillin/streptomycin were used to grow Human Embryonic Kidney HEK293T cells and K562 cells, respectively (purchased from ATCC). Cells were maintained at 37 °C with 5% CO_2. These cell lines have been tested for mycoplasma contamination routinely by using GeneCopoeia (catalog no. MPD-T-050), and they have given negative results.

Transient transfections and auxin treatment

Around 60%–70% confluent cells in 10-cm plates were used for the transient transfection in the presence of Promega FuGene6 (catalog no. E2691) transfection reagent according to the manufacturer's protocol. Three separate 10-cm plates were harvested for each HA-ChIP, and two plates were harvested for each H3K27Ac ChIP. For the Auxin treatment, 3-indoleacetic acid was purchased from Sigma (catalog no. I2886) and solubilized in 100% EtOH before each treatment as a fresh solution. Cells were treated with 1 mM Auxin at the designated time point. Transfected cells were harvested after 72 h for the ChIP assay and Q-PCR. For auxin-treated cells, auxin treatment was initiated after 72 h and all samples were collected at the same time. Same molar ratios of plasmids were used for the dCas9–p300 and pooled sgRNA. In the case of degron study, AID-containing plasmid (AID–dCas9–p300) was used instead of dCas9–p300 in 293T-TIR stable cell lines. OsTIR expression was induced by 1 mg/ml doxycycline.

sgRNA design

Only sgRNA expressing plasmid was derived from an original plasmid (Addgene no. 42230) after PstI digestion and self-ligation. Each sgRNA sequence was chosen according to the CrisprScan [47] and CROP-IT tools [48], and their first nucleotide was modified to the "G" if it is not. "CACC" overhangs were added to the 5′ of the forward oligo and "AAAC" overhangs were added to the 5′ of reverse complementary oligo for each sgRNA. Two oligos were heated to the 95 °C and cooled down gradually in PCR machine. Annealed oligos were ligated into Bbs.i (NEB catalog no. R0539) cut plasmid. For each region, four different sgRNAs were prepared and mixed with equal molar ratios after the sequence confirmation. All target sgRNA sequences were listed in Supplementary Table 1.

Plasmids

dCas9–p300 and dCas9–p300(D1399Y) plasmids were kind gifts from Dr. Charles Gersbach's laboratory (Duke University). They are also available from Addgene with following the catalog numbers 61357 and 61358. dCas9–p300 plasmid was digested with SacII to insert the AID peptide at the N-termini of the fusion protein. Sanger sequencing confirmed the direction of AID.

Chromatin immunoprecipitation

Two or three 10-cm plates of 293T cells were used in each ChIP experiment according to the previous protocol [49]. Briefly, 1% formaldehyde (Sigma, catalog no. F8775) was used for the crosslinking of the cells for 10 min at 37 °C, and 0.125 M glycine (final concentration) for 5 min was used for quenching the effect of excess formaldehyde. Crosslinked cells were washed with cold PBS twice. Add 1 tablet of protease inhibitor (Roche, catalog no. 11836153001) immediately before use to the SDS lysis buffer [100 mM NaCl, 50 mM Tris–Cl (pH 8.1), 5 mM EDTA and 1% (wt/vol) SDS] and lyse the cells in this buffer with 20-min incubation on ice. Branson digital sonifier was used for the sonication with the following program: 9 min at 40% amplitude with 0.7-s "on" and 1.3-s "off" pulse cycles. Then, dilute the sonicated lysates 10 times by using ChIP-dilution buffer [0.01% SDS, 1.1% Triton X-100, 1.2 mM EDTA, and 16.7 mM Tris–HCl (pH 8.1)], and add 1.5 μg HA-ChIP grade antibody (abcam no. 9110) or 2 μg H3K27Ac ChIP-grade antibody (abcam no. 4729) for overnight incubation at 4 °C. Next day, add 30-μl mixtures of protein A–G magnetic beads (Dynabeads, Life Technologies) to the lysates and rotate for 2 h at 4 °C. DNA–antibody–protein A/G complex of beads was washed two times of each of the following buffer. (1) low-salt immune complex wash buffer [0.1% SDS, 1% Triton X-100, 2 mM EDTA, 20 mM Tris–HCl (pH 8.1), and 150 mM NaCl], (2) LiCl wash buffer [0.25 M LiCl, 1% NP40, 1% deoxycholate, 1 mM EDTA, and 10 mM Tris–HCl (pH 8.1)], and (3) TE [10 mM Tris–HCl and 1 mM EDTA (pH 8.0)]. The DNA–protein complex was recovered from the beads by 30-min incubation with elution buffer (0.2% SDS and 0.1 M $NaHCO_3$ supplemented with fresh 5 mM DTT) at 65 °C. Incubate the samples at 65 °C for another 6 h, which is followed by 2 h of proteinase K treatment (Amresco, 20 mg/ml) for the reverse cross-linking process. DNA was extracted

with cold-ethanol precipitation method and quantified with Qubit Fluorometer.

RT-qPCR for mRNA levels

RNA from transfected cells was harvested with RNeasy Plus Mini Kit (Qiagen catalog no. 74134) according to the manufacturer's protocol. One microgram of RNA was converted into cDNA by using AB high capacity RNA-to-cDNA kit (catalog no. 4387406). Oligos used for the qRT-PCR were listed in Supplementary Table 2. HPRT-1 gene was used as an internal control for each analysis.

qPCR for ChIP DNA

To understand the function of dCas9–p300 binding on their target site, two primer pairs spanning the target sites were used to analyze the H3K27ac enrichment level, and one primer inside the target site of the sgRNA-pool area was used to analyze the dCas9 (p300) fold enrichment. Chip primer sequences for each locus were summarized in Supplementary Table 3. The ΔΔCt method by using IP DNA and whole-cell extract DNA was used together with target ChIP primers and nomod control primer to calculate the fold enrichment ratios for each locus. Nomod (no modification) control primer sequences are as follows:

nomod-for: 5′-AAAAATCAGTTTGTGTGTTTGTGG
nomod-rev: 5′-CCTAGGCAACAGTGACACCTATTT

Luciferase assay

sgRNA target sites were amplified with primers listed in Supplementary Table 4. After PCR amplification of each 300-bp fragment, NheI (NEB) and XhoI (NEB) enzymes were used to digest the PCR products. Since IL1RN promoter sequence has internal NheI cutting site, only this fragment was inserted into a vector by blunt end ligation after SmaI cut. pGL3 plasmids (basic and promoter) were also digested with the same set of enzymes and used as a vector to put the digested insert via T4 DNA ligase (NEB). 293T cells were transfected with 100:1 ratio of Luciferase/Renilla plasmids and harvested after 2 days of infection. Luciferase and Renilla activities were measured by using Dual-Luciferase Reporter Assay System (Promega catalog no. E1910) according to the manufacturer's protocol.

3C assay

3C experiment was performed as stated in Hagege *et al*. [50]. Briefly, 10 million HEK-293T cells were collected and crosslinked with 2% formaldehyde/10% FCS/PBS. Crosslinking was quenched with 1 M glycine. Sequentially, cell and nuclear membrane lysis reactions were performed with appropriate buffers. Overnight restriction digestion with NlaIII enzyme was carried out. Samples were taken from lysis solution before and after digestion to check for the efficiency of digestion. Ligation was carried out by using T4 Ligase. Proteins on interacting sites were degraded with proteinase K. RNA contamination was removed by RNase. DNAs were precipitated with phenol–chloroform, and qPCR was performed by using complementary primers to suspected interacting sites. 3C ratio was calculated by using C_t value difference between A, B, and C primer pairs and genomic nomod control primer. Then, iEs target sgRNAs of the WT and mut p300 3C values were normalized to the control sgRNA-infected cells. Primer sequences used in this assay were shown in Supplementary Table 5.

Supplementary data to this article can be found online at https://doi.org/10.1016/j.jmb.2018.08.001.

Acknowledgement

We thank Dr. Charles Gersbach for sharing the dCas9–P300 plasmids. The research was partially funded through a pilot project (NIDDK P50 DK096373), V Scholar award to M.A. from V Cancer Research Foundation, and UVA Cancer center pilot project awards to M.A. Additional funding came from National Science Foundation (MCB 1715183).

Author Contributions: M.A. and C.K. designed the study; C.K. together with R.M., A.C., H.U., and S.A. performed experiments. M.K. designed the original AID plasmids. S.B. contributed to the mathematical formulation of the results.

Conflict of Interest Statement: The authors declare no conflict of interest.

Received 1 May 2018;
Received in revised form 26 July 2018;
Accepted 1 August 2018
Available online 9 August 2018

Keywords:
CRISPR;
non-regulatory regions;
AID (auxin-inducible degron);
enhancer-like elements;
p300

Abbreviations used:
sgRNA, short-guide RNA; dCas9, catalytically inactive Cas9; AID, auxin-inducible degron; HAT, histone acetyl transferase; H3K27ac, histone 3 at lysine 27 position; iE, induced Enhancer.

References

[1] G.A. Maston, S.K. Evans, M.R. Green, Transcriptional regulatory elements in the human genome, Annu. Rev. Genomics Hum. Genet. 7 (2006) 29–59.

[2] Y. Atlasi, H.G. Stunnenberg, The interplay of epigenetic marks during stem cell differentiation and development, Nat. Rev. Genet. 18 (11) (2017) 643–658.

[3] E.P. Consortium, et al., An integrated encyclopedia of DNA elements in the human genome, Nature 489 (7414) (2012) 57–74.

[4] Roadmap Epigenomics, C, et al., Integrative analysis of 111 reference human epigenomes, Nature 518 (7539) (2015) 317–330.

[5] C.M. Rivera, B. Ren, Mapping Human Epigenomes, Cell 155 (1) (2016) 39–55.

[6] J. Zhu, et al., Genome-wide chromatin state transitions associated with developmental and environmental cues, Cell 152 (3) (2013) 642–654.

[7] A.P. Feinberg, Phenotypic plasticity and the epigenetics of human disease, Nature 447 (7143) (2007) 433–440.

[8] U.C. Lange, R. Schneider, What an epigenome remembers, BioEssays 32 (8) (2010) 659–668.

[9] S.B. Baylin, P.A. Jones, A decade of exploring the cancer epigenome—biological and translational implications, Nat. Rev. Cancer 11 (10) (2011) 726–734.

[10] H. Shen, P.W. Laird, Interplay between the cancer genome and epigenome, Cell 153 (1) (2013) 38–55.

[11] P.I. Thakore, et al., Editing the epigenome: technologies for programmable transcription and epigenetic modulation, Nat. Methods 13 (2) (2016) 127–137.

[12] M. Jinek, et al., A programmable dual-RNA-guided DNA endonuclease in adaptive bacterial immunity, Science 337 (6096) (2012) 816–821.

[13] P. Mali, et al., RNA-guided human genome engineering via Cas9, Science 339 (6121) (2013) 823–826.

[14] L. Cong, et al., Multiplex genome engineering using CRISPR/Cas systems, Science 339 (6121) (2013) 819–823.

[15] L.S. Qi, et al., Repurposing CRISPR as an RNA-guided platform for sequence-specific control of gene expression, Cell 152 (5) (2013) 1173–1183.

[16] A.W. Cheng, et al., Multiplexed activation of endogenous genes by CRISPR-on, an RNA-guided transcriptional activator system, Cell Res. 23 (10) (2013) 1163–1171.

[17] P. Perez-Pinera, et al., RNA-guided gene activation by CRISPR–Cas9-based transcription factors, Nat. Methods 10 (10) (2013) 973–976.

[18] B. Chen, et al., Dynamic imaging of genomic loci in living human cells by an optimized CRISPR/Cas system, Cell 155 (7) (2013) 1479–1491.

[19] P. Qin, et al., Live cell imaging of low- and non-repetitive chromosome loci using CRISPR–Cas9, Nat. Commun. 8 (2017) 14725.

[20] L.A. Gilbert, et al., Genome-scale CRISPR-mediated control of gene repression and activation, Cell 159 (3) (2014) 647–661.

[21] I.B. Hilton, et al., Epigenome editing by a CRISPR–Cas9-based acetyltransferase activates genes from promoters and enhancers, Nat. Biotechnol. 33 (5) (2015) 510–517.

[22] P.I. Thakore, et al., Highly specific epigenome editing by CRISPR–Cas9 repressors for silencing of distal regulatory elements, Nat. Methods 12 (12) (2015) 1143–1149.

[23] N.A. Kearns, et al., Functional annotation of native enhancers with a Cas9–histone demethylase fusion, Nat. Methods 12 (5) (2015) 401–403.

[24] A. Vojta, et al., Repurposing the CRISPR–Cas9 system for targeted DNA methylation, Nucleic Acids Res. 44 (12) (2016) 5615–5628.

[25] T. Kouzarides, Chromatin modifications and their function, Cell 128 (4) (2007) 693–705.

[26] C.T. Ong, V.G. Corces, Enhancers: emerging roles in cell fate specification, EMBO Rep. 13 (5) (2012) 423–430.

[27] M. Bulger, M. Groudine, Functional and mechanistic diversity of distal transcription enhancers, Cell 144 (3) (2011) 327–339.

[28] E. Calo, J. Wysocka, Modification of enhancer chromatin: what, how, and why? Mol. Cell 49 (5) (2013) 825–837.

[29] A. Rada-Iglesias, et al., A unique chromatin signature uncovers early developmental enhancers in humans, Nature 470 (7333) (2011) 279–283.

[30] R.E. Thurman, et al., The accessible chromatin landscape of the human genome, Nature 489 (7414) (2012) 75–82.

[31] D. Hnisz, et al., Super-enhancers in the control of cell identity and disease, Cell 155 (4) (2013) 934–947.

[32] D. Hnisz, et al., Convergence of developmental and oncogenic signaling pathways at transcriptional super-enhancers, Mol. Cell 58 (2) (2015) 362–370.

[33] G. Korkmaz, et al., Functional genetic screens for enhancer elements in the human genome using CRISPR–Cas9, Nat. Biotechnol. 34 (2) (2016) 192–198.

[34] W.A. Flavahan, et al., Insulator dysfunction and oncogene activation in IDH mutant gliomas, Nature 529 (7584) (2016) 110–114.

[35] M. Delvecchio, et al., Structure of the p300 catalytic core and implications for chromatin targeting and HAT regulation, Nat. Struct. Mol. Biol. 20 (9) (2013) 1040–1046.

[36] J. Dekker, et al., Capturing chromosome conformation, Science 295 (5558) (2002) 1306–1311.

[37] T. Fujita, H. Fujii, Efficient isolation of specific genomic regions and identification of associated proteins by engineered DNA-binding molecule-mediated chromatin immunoprecipitation (enChIP) using CRISPR, Biochem. Biophys. Res. Commun. 439 (1) (2013) 132–136.

[38] C. Kuscu, et al., Genome-wide analysis reveals characteristics of off-target sites bound by the Cas9 endonuclease, Nat. Biotechnol. 32 (7) (2014) 677–683.

[39] K. Nishimura, et al., An auxin-based degron system for the rapid depletion of proteins in nonplant cells, Nat. Methods 6 (12) (2009) 917–922.

[40] A.J. Holland, et al., Inducible, reversible system for the rapid and complete degradation of proteins in mammalian cells, Proc. Natl. Acad. Sci. U. S. A. 109 (49) (2012) E3350–E3357.

[41] L. Bintu, et al., Dynamics of epigenetic regulation at the single-cell level, Science 351 (6274) (2016) 720–724.

[42] D. Balboa, et al., Conditionally stabilized dCas9 activator for controlling gene expression in human cell reprogramming and differentiation, Stem Cell Rep. 5 (3) (2015) 448–459.

[43] S.M.G. Braun, et al., Rapid and reversible epigenome editing by endogenous chromatin regulators, Nat. Commun. 8 (1) (2017) 560.

[44] B. Chen, et al., Expanding the CRISPR imaging toolset with *Staphylococcus aureus* Cas9 for simultaneous imaging of multiple genomic loci, Nucleic Acids Res. 44 (8) (2016) e75.

[45] S. Shao, et al., Long-term dual-color tracking of genomic loci by modified sgRNAs of the CRISPR/Cas9 system, Nucleic Acids Res. 44 (9) (2016) e86.

[46] S.L. Morgan, et al., Manipulation of nuclear architecture through CRISPR-mediated chromosomal looping, Nat. Commun. 8 (2017) 15993.
[47] M.A. Moreno-Mateos, et al., CRISPRscan: designing highly efficient sgRNAs for CRISPR–Cas9 targeting in vivo, Nat. Methods 12 (10) (2015) 982–988.
[48] R. Singh, et al., Cas9–chromatin binding information enables more accurate CRISPR off-target prediction, Nucleic Acids Res. (2015) 43(18).
[49] M. Adli, J. Zhu, B.E. Bernstein, Genome-wide chromatin maps derived from limited numbers of hematopoietic progenitors, Nat. Methods 7 (8) (2010) 615–618.
[50] H. Hagege, et al., Quantitative analysis of chromosome conformation capture assays (3C-qPCR), Nat. Protoc. 2 (7) (2007) 1722–1733.